

*THE SPECTRUM AND TEMPORAL CHARACTERISTICS OF STIMULATED EMISSION IN  
CaF<sub>2</sub>:Sm<sup>2+</sup>*

Yu. A. ANAN'EV and B. M. SEDOV

Submitted to JETP editor May 19, 1964

J. Exptl. Theoret. Phys. (U.S.S.R.) 48, 782-790 (March, 1965)

The spectrum of the stimulated radiation from CaF<sub>2</sub>:Sm<sup>2+</sup> is investigated experimentally. Distribution of the radiation with respect to axial oscillation modes is studied. A continuous replacing of transverse oscillation modes has been observed under steady state emission conditions. It is demonstrated that the absence of oscillations in the integrated radiation from CaF<sub>2</sub>:Sm<sup>2+</sup> is due to superposition of a large number of spikes over a certain period of time, the spikes being due to various transverse modes of oscillations. Information on the spatial distribution of various oscillation modes in the radiation has been obtained.

## 1. INTRODUCTION

At present, to obtain stimulated emission in the optical region, resonators are used which as a rule have a large number of modes within the fluorescence line of the active medium. The mechanisms for the production and interaction of the various types of modes in these resonators are very complicated. As a result many of the effects that have been observed in studies of the spectral and temporal properties of stimulated emission have not yet received even qualitative explanations. In particular there are a number of unanswered questions concerning the "spiked" character of stimulated emission, which persists even under long-term continuous excitation of the active medium<sup>[1]</sup>. The study of stimulated emission in CaF<sub>2</sub>:Sm<sup>2+</sup> is of interest in this connection, since this substance seems to be at present the only solid state active medium for which spiking is not observed in laser emission. For stimulated emission in CaF<sub>2</sub>:Sm<sup>2+</sup>, the short luminescence lifetime ( $1 - 2 \times 10^{-6}$  sec<sup>[2,3]</sup>) results in very short duration for the transient processes which frequently complicate the interpretation of the experimental data.

A significant advantage of this active medium is its high optical uniformity, which makes possible simple classification of the modes observed in stimulated emission.

The theory of resonators with plane ends (cf. for example,<sup>[4]</sup>) or ends which are approximately plane (<sup>[5]</sup>) predicts, for the case of not too long a cavity length  $l$ , a grouping of the frequencies of the lowest order modes around the values  $m_1 c / 2\kappa l$ , where  $\kappa$  is the index of refraction and  $m_1$  is an integer (the axial index). In the present work we

used rods 8 mm in diameter and 20 mm long, with ends parallel to 3" of arc and flat to 0.2 fringe; index of refraction variations were essentially absent in the rods used. Rough estimates similar to those made in the paper of Leontovich and Veduta<sup>[6]</sup> indicate that under these conditions the spectral interval between modes with the same axial index should be approximately two orders of magnitude smaller than the interval between modes with different axial index. Preliminary investigation<sup>[7]</sup> using the above rods indicated that the spectrum of the stimulated emission consists in fact of a series of sharp, equally spaced bands, whose separation is constant and equal to  $c/2\kappa l$  ( $\Delta\lambda = 0.088 \text{ \AA}$ ). Thus the observed bands may be identified with groups of modes having the same axial index<sup>1)</sup>. This allows us to use the very simple model set forth in<sup>[8,9]</sup> in analyzing the experimental data.

## 2. EXPERIMENTAL METHODS

The optical set-up is shown in Fig. 1. The source of stimulated emission to be studied consisted of a sample of CaF<sub>2</sub>:Sm<sup>2+</sup> with reflecting coatings on its ends; the rod was cooled by helium gas.

The spectral analysis was made with a Fabry-Perot etalon having a mirror reflectivity not less than 99.5% at 0.7  $\mu$ . This very high reflectivity and the extremely accurate preparation of the mirrors, in conjunction with the extremely high (in comparison to classical spectrographic sources) brightness of the radiation being investigated,

<sup>1)</sup>For an active medium made of very inhomogeneous material this classification may be more difficult (cf., e.g., <sup>[6]</sup>).

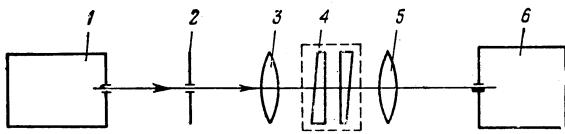


FIG. 1. Optical set-up: 1—Emission source, 2—slit, 3 and 5—lenses, 4—Fabry-Perot etalon, 6—mechanical camera.

allows one to obtain very large spectral resolution for relatively short etalon lengths. In fact, for the case of very large reflectivities, the usual limitation on resolving power of the etalon is the error in the preparation of the mirrors. Because of the high brightness of the stimulated emission, it is possible to record the spectrum using very small angles of incidence and a very small entrance pupil at the input to the etalon; this significantly decreases the effects of errors in preparing the mirrors<sup>[10]</sup>. In the present work a beam with a  $3 \times 6$  mm cross-section was directed at the portion of the etalon with the smallest local errors; only a portion of the zeroth order was detected. Under these conditions the spectral resolving power was usually about  $1/150$ – $1/250$  of the separation between neighboring orders; the resolving power in the center of the zeroth order was  $1/400$  of the inter-order separation. Thus in Fig. 4a the largest angular radius of the etalon rings is  $7.8 \times 10^{-3}$ , corresponding to a spectral range of  $0.215 \text{ \AA}$ , whereas the separation between neighboring orders is  $0.313 \text{ \AA}$ . The average separation between single spectral components in this picture is  $2\text{--}3 \times 10^{-3} \text{ \AA}$ , the smallest is of the order of  $1 \times 10^{-3} \text{ \AA}$ .

In order to record the temporal development of the stimulated emission we used a mechanical camera with a film rotation rate of  $0.08 \text{ mm}/\mu\text{sec}$ . In this case, (Fig. 1), we used the lens 5 ( $f = 800 \text{ mm}$ ) to project onto the film, in addition to the etalon rings, an image of the slit located in the focal plane of the lens 3 ( $f = 300 \text{ mm}$ ). In most of the experiments the slit width was  $0.02 \text{ mm}$  and the time resolution was  $0.8 \mu\text{sec}$ . To observe the time integrated spectrum of the output the slit was omitted.

### 3. SPECTRAL DISTRIBUTION OF THE LASER OUTPUT

The distribution of the laser output intensity among the various spectral bands is of particular interest, since comparison of the actual distribution with the results of theoretical estimates gives information on the nature of the broadening of the fluorescence line, on the spatial and spectral diffu-

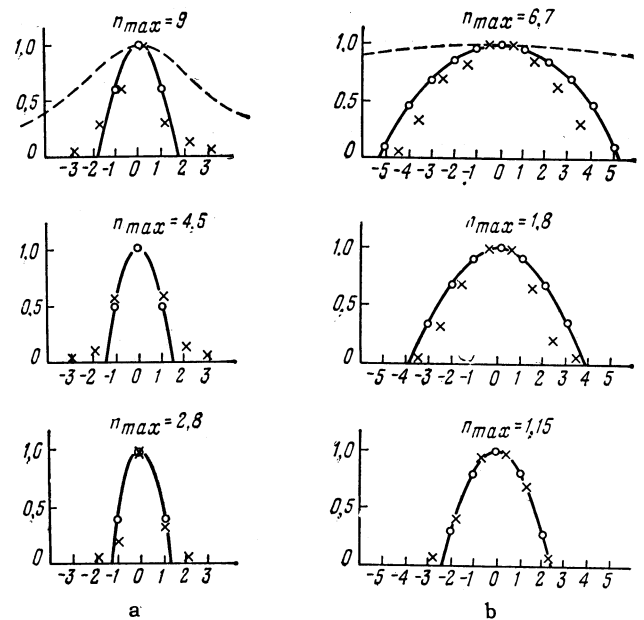


FIG. 2. Distribution of the stimulated emission intensity among the spectral bands as a function of  $\Delta\nu / (c/2\kappa l)$ . Temperature of the sample is: a— $10^\circ\text{K}$ , b— $40^\circ\text{K}$ . The crosses are experimental data (the time integrated emission intensities from individual spectral bands, in arbitrary units), the circles are calculated values and the dotted lines give the fluorescence line shape.

sion of excitation, etc. (cf. for example, <sup>[11,9]</sup>). In the present work we made measurements of spectral distribution for  $\text{CaF}_2:\text{Sm}^{2+}$  by recording the time integrated stimulated emission spectrum, followed by photometric measurements on the plates.

The base of the Fabry-Perot etalon in the present experiments was  $1 \text{ mm}$ , and the temperature of the sample was either  $15$  or  $40^\circ\text{K}$ . The pumping pulse was bell-shaped and was weak enough so that sample heating due to the pump radiation was essentially absent. The results of the measurements are shown in Fig. 2. The spectral width of the band over which the stimulated emission is distributed increases with increasing pump power above threshold, proportional to the pump intensity  $n$ ; the same is true with increasing temperature. For  $15^\circ\text{K}$  the width was  $0.2\text{--}0.3 \text{ \AA}$ , whereas for  $40^\circ\text{K}$  it was  $0.5\text{--}0.7 \text{ \AA}$ . Moreover, investigation of the line shape using the Fabry-Perot etalon showed a Lorentz line whose half-width  $\Delta\lambda_L$  in the temperature range  $10\text{--}77^\circ\text{K}$  was proportional to  $T^2$  (cf. Fig. 3); it was  $0.6 \text{ \AA}$  for  $15^\circ\text{K}$ , and  $4 \text{ \AA}$  for  $40^\circ\text{K}$ <sup>2)</sup>. Thus even for comparatively large excess

<sup>2)</sup>Measurements of the value of  $\Delta\lambda_L$  in the temperature range  $20\text{--}77^\circ\text{K}$  essentially coincide with the data of Kaiser et al.<sup>[3]</sup>; their results for measurements of  $\Delta\lambda_L$  at  $4^\circ\text{K}$  are somewhat too high.

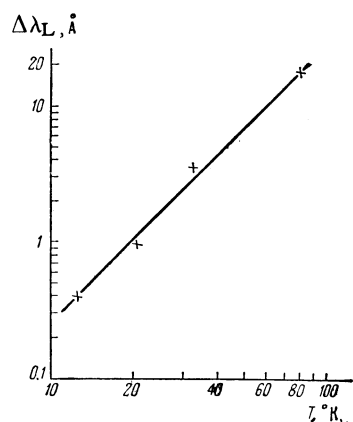


FIG. 3. Dependence of the half-width of the fluorescence line on temperature: the crosses are experimental points, the straight line corresponds to a quadratic dependence of  $\Delta\lambda_L$  on  $T$ .

pumping excitation, the stimulated emission is concentrated in a narrow spectral band close to the peak of the fluorescence line.

The above fact indicates that the fluorescence line is homogeneously broadened<sup>3)</sup>, since inhomogeneous broadening coupled with any significant excess of pumping above threshold leads to a larger spectral width of the stimulated emission<sup>[11]</sup>. The validity of this conclusion about the nature of the broadening of the active transition in  $\text{CaF}_2:\text{Sm}^{2+}$  is supported by comparing the actual distribution of the stimulated emission intensity with the distribution obtained by calculations for the case of simple homogeneous line broadening. This calculation was made using the assumptions of Tang et al.<sup>[9]</sup>; this method is extended to the case of pumping far above threshold (cf. the Appendix). The effect of the non-uniform distribution of pump intensity throughout the cross section of the rod, and the deviation of the pump pulse shape from rectangular were taken care of by the following approximation; the experimentally measured ratio of the maximum pump power to the threshold ( $n_{\text{max}}$ ) is replaced in the calculations by an effective value of excess above threshold, viz.,  $(1/2)(1 + n_{\text{max}})$ . Considering the crudeness of these estimates, the agreement between the experimental data and the results of the calculation (cf. Fig. 2) may be considered satisfactory. The rather weak wings of the actual distribution at 15°K obviously may be explained by a distribution of  $Q$  values for the modes of the real cavity.

<sup>3)</sup>For a definition of this concept see<sup>[11]</sup>. A possible mechanism for homogeneous broadening in  $\text{CaF}_2:\text{Sm}^{2+}$  is described in<sup>[12]</sup>.

#### 4. THE FINE STRUCTURE OF THE SPECTRUM

The spectral resolution necessary for observing single modes was achieved by increasing the length of the etalon, depending on the length of the laser rod being used, so that for the longer etalon the successive orders are equally spaced rings corresponding to the separate spectral bands, and so that in successive orders one records similar systems of rings. Since one knows the spectral intervals between neighboring bands (cf.<sup>[7]</sup>) and between the orders of the etalon, the interpretation of these spectrograms was not difficult.

In Fig. 4a we show one such spectrogram. Consideration of this picture shows that each spectral band about 0.02 Å wide contains several modes having constant separation. The duration of the contribution of a particular mode to the stimulated emission does not exceed 10 μsec.

Decreasing the pump intensity causes a narrowing of spectral bands (usually their width is from 0.02 to 0.005 Å) accompanied by a decrease in the number of individual modes; the duration of each of the modes in these bands increases (Fig. 4b, c). This behavior was observed both in the most intense bands and in the bands farthest from the center of the fluorescence line.

On the other hand, increasing the temperature of the sample for constant pump intensity gives rise to a decrease in the duration of the emission corresponding to individual modes (Fig. 4d); when the total stimulated emission output is recorded with a photomultiplier this change results in a continuous change from the stationary regime to the spiking regime (cf. Fig. 5). Thus, in agreement with the conclusions of Kaiser et al.<sup>[3]</sup>, the presence of spikes in the output of  $\text{CaF}_2:\text{Sm}^{2+}$  is difficult to observe because of their overlapping in time rather than the insufficient time resolution in the detection system.

The displacement of the spectral bands towards longer wavelengths which occurs at the end of the pump pulse is explained by the heating of the sample. The magnitude of the displacement corresponds to the results of direct measurements of the sample deformation<sup>[13]</sup>.

To explain the influence of thermal effects on the succession of modes, a comparison was made of spectrograms obtained for various rates of sample heating due to pump radiation. The remaining experimental conditions, in particular the stimulated emission power, were not changed (to ensure similar conditions use was made of the dependence of the magnitude of the Stokes losses on the spectral composition of the pumping radiation). Varia-

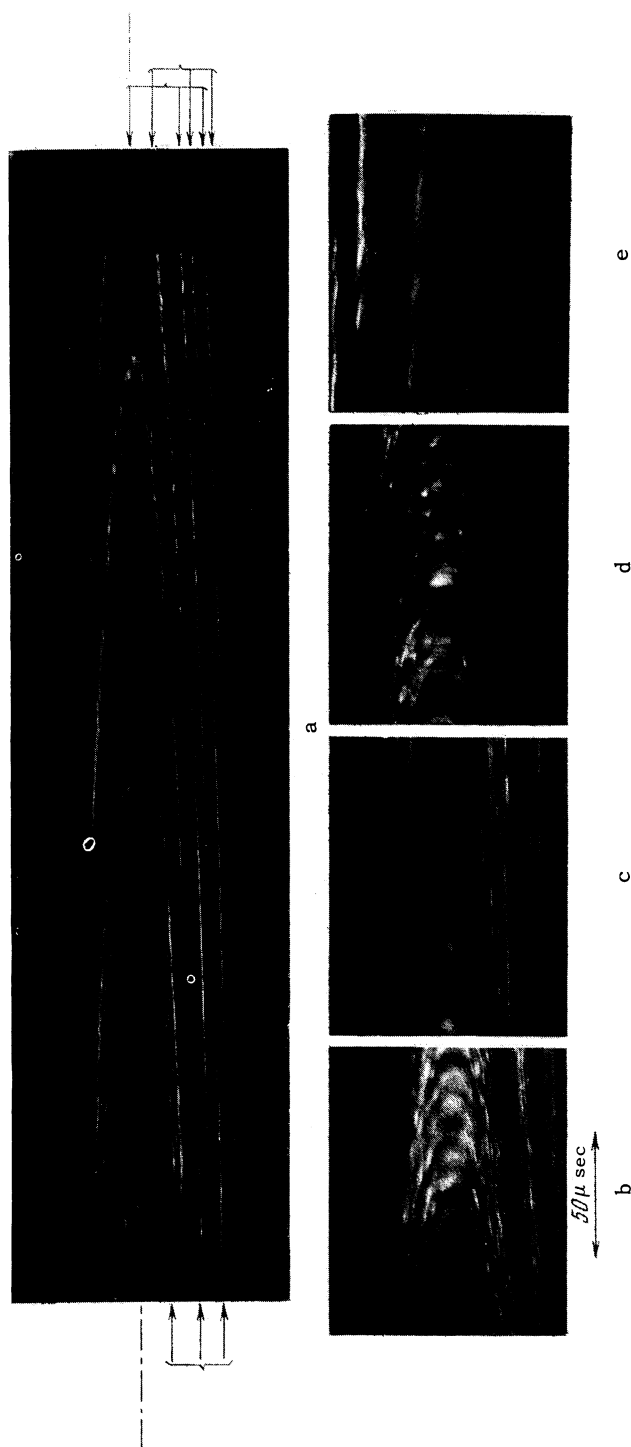


FIG. 4. Time sweep of the stimulated emission for excitation of the sample by a rectangular shaped pulse. The direction of the time development is from left to right, and the time resolution is about  $1 \mu\text{sec}$ . a — the initial temperature of the sample is  $T = 20^\circ\text{K}$ , the duration of the flash lamp pulse is  $700 \mu\text{sec}$ , and the base of the etalon is  $t = 8 \text{ mm}$ . The horizontal axis corresponds to the center of the ring pattern of the etalon. Three orders of the etalon are superposed. The images of bands corresponding to a given order are shown by brackets; b —  $T = 20^\circ\text{K}$ ,  $t = 25 \text{ mm}$ ; c — the same as in b, the flash lamp intensity has been decreased by a factor of 3; d —  $T = 45^\circ\text{K}$ ; the other conditions are the same as in b, e —  $T = 20^\circ\text{K}$ ,  $t = 8 \text{ mm}$ .

tion of the thermal output by a factor of from 1.5 to 3 caused no observable variations in the details of the succession of the various modes.

During an individual spike the frequency of a given mode varied with the thermal expansion of the cavity (cf. Fig. 4); no mismatch between the emission frequencies and the frequencies of the cavity modes occurred.

The succession of modes is also difficult to explain on the basis of transient processes or the basis of non-uniform pumping, since the duration of the pumping pulse is extremely long in comparison to the length of the transient processes in  $\text{CaF}_2:\text{Sm}^{2+}$ ; moreover the shape of the pump pulse is very close to rectangular (the discharge curve was an artificial line made up of 16 sections).

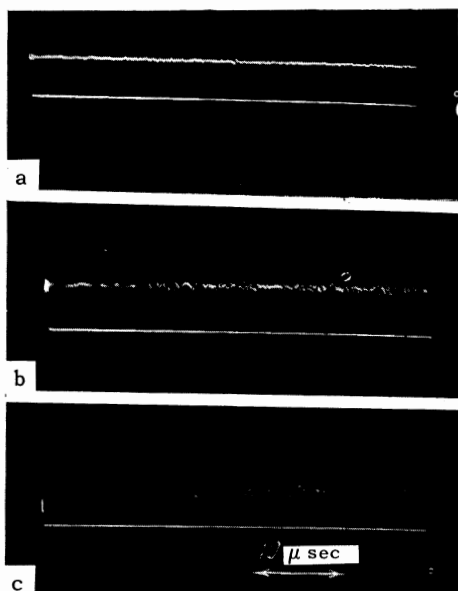


FIG. 5. Oscillogram of the total stimulated emission intensity; a -  $T = 25^\circ\text{K}$ , b -  $T = 50^\circ\text{K}$ , c -  $T = 60^\circ\text{K}$ .

Hence it is natural to propose that, contrary to widespread opinion (cf. [14]), the successive replacement of the modes may reflect a self-excited oscillatory behavior which is inherent in the stationary regime of laser action in  $\text{CaF}_2:\text{Sm}^{2+}$ . In the general case this replacement is probably caused by the formation of "holes" (using the terminology of Bennet [11]) in the fluorescent line shape due to inhomogeneous broadening, and the resulting instantaneous decrease in the number of excited atoms in localized regions of the greatest intensity for a particular type of mode.

A consequence of a decrease in the number of excited atoms in particular regions of the cavity is the preferential excitation in the following instants of time of well-defined modes which are localized primarily outside these regions. Thus spatial effects may cause the regularity in the replacement and succession of the modes. Observation of this regularity (cf. Fig. 4e and also [15]) underlines the importance of spatial effects in the kinetics of laser action.

In the case of  $\text{CaF}_2:\text{Sm}^{2+}$ , the spectral "holes" which can prevent the simultaneous existence of modes with closely spaced frequencies evidently do not appear; this is clearly related to the nature of the fluorescence line broadening.

## 5. SPATIAL DISTRIBUTION OF THE EMISSION

To study the spatial distribution of the radiation in single modes we projected onto the film, in addition to the fringes from the etalon, an image of the end face of the sample or, alternatively, the far



FIG. 6. The time-integrated emission spectrum: a - the image of the end face of the sample is superposed on the image of the etalon ring; b - the far field pattern of the emission is superposed on the ring pattern of the etalon.

field distribution of the radiation. In Fig. 6 we show photographs of the time-integrated emission spectrum obtained for pump pulses so short (about  $5 \mu\text{sec}$ ) that the total number of modes present is small and the temperature drift of the frequencies is negligibly small. A single ring in these photographs corresponds to a single mode. It is not difficult to conclude that the emission of each mode occupies a considerable fraction of the end face of the sample and of the solid angle of laser action (otherwise we would not have observed complete rings but rather only a small illuminated arc). These same conclusions, which confirm the results of Leontovich, Veduta and Korobkin [16,6], result from an analysis of time sweeps of the spectrum obtained under suitable conditions. In view of the considerable angular separation between the emission from various modes and the extremely large spectral interval between them<sup>4)</sup> (about  $0.002 \text{ \AA}$ ) one may conclude that, due to the imperfections in the sample, the modes observed in this work do not coincide with the modes of an ideal cavity.

<sup>4)</sup>In our case for a sample diameter of 8 mm we find that, for the first nine modes of the ideal cylindrical cavity with plane parallel ends, the maximum separation in wavelength should be about  $2.5 \times 10^{-5} \text{ \AA}$  [17].

6. CONCLUSION

The results of these investigations of the spectral and temporal character of the  $\text{CaF}_2:\text{Sm}^{2+}$  emission show that many of the actual properties of the stimulated emission are well understood within the framework of the well-known theoretical ideas. Thus the stimulated emission spectrum of a rod with plane parallel ends is divided into a series of bands corresponding to groups of modes with the same axial index. The distribution of the stimulated emission intensity among these bands is satisfactorily described by the relationships obtained by Tang et al.<sup>[9]</sup> Finally, small deviations in the shape of the cavity from the ideal lead to significant modifications of the modes (cf. also<sup>[6,18]</sup> and others). An estimate similar to that given by Leontovich and Veduta<sup>[6]</sup> leads to the conclusion that the average spectral interval between single modes corresponds satisfactorily to the errors in fabrication of the cavity.

We do not yet have an explanation for the spiking behavior of laser action in  $\text{CaF}_2:\text{Sm}^{2+}$  which is observed to accompany prolonged and essentially constant pumping. The mechanism which gives rise to the self-oscillatory behavior of the processes which occur in the cavity requires explanation (put differently, there is need for an explanation of the cause of the non-stationary type of excitation observed under the above-described conditions).

The authors express their deep thanks to A. A. Mak for suggesting this problem, for valuable advice, and for discussion of the results.

APPENDIX

CALCULATION OF THE SPECTRAL DISTRIBUTION OF THE OUTPUT INTENSITY

For the stationary state in a four-level laser with the terminal state of the working transition empty, the conditions for stationarity for  $(2r + 1)$  spectral bands symmetrically arranged with respect to the fluorescence line center are, according to<sup>[9,14]</sup>, written in the form

$$\frac{d \ln A_i}{dt} \sim \int_0^1 \frac{ng_i(1 - \cos 2\pi m_i x) dx}{1 + \sum g_k A_k (1 - \cos 2\pi m_k x)} - 1 \begin{cases} = 0, & i = 0, \pm 1, \dots, \pm r \\ < 0, & |i| > r \end{cases} \quad (1)$$

where  $n$  is the excess pump power above laser threshold;  $m_i = m_0 + i$  is the number of wavelengths  $\lambda_i$ , which are contained in twice the cavity length;  $i$  is the number of the spectral band (at the center

$i = 0$ );  $g_i = g(\lambda_i)$ ,  $g(\lambda)$  is the fluorescence line shape;  $g_0 = 1$ ; and  $A_i$  is the total scattered energy of the modes belonging to the  $i$ -th band (including the power which leaves the cavity) in units of the fluorescence power at threshold.

In all formulas the summation is over the index  $k$  from  $-r$  to  $+r$ .

We expand the factor  $n[1 + \sum g_k A_k (1 - \cos 2\pi m_k x)]^{-1}$  in a series; (this factor describes the population distribution of the excited atoms in units of the population at threshold), and we obtain

$$\frac{1}{1 + \sum A_k' (1 - \cos 2\pi m_k x)} = \frac{1}{1 + \sum A_k'} + \frac{\sum A_k' \cos 2\pi m_k x}{(1 + \sum A_k')^2} + \frac{(\sum A_k' \cos 2\pi m_k x)^2}{(1 + \sum A_k')^3} + \dots, \quad A_{-k}' = A_k' \equiv g_k A_k.$$

Limiting ourselves to the above terms in the expansion<sup>5)</sup> we obtain after cumbersome but straightforward calculations

$$A_i' = 2 \left( 1 + \sum A_k' \right)^2 \times \left\{ z_i - \frac{\sum z_k / g_k}{\sum 1/g_k + n/2 \left( 1 + \sum A_k' \right)^2} \right\}, \quad (2)$$

$i = 0, \pm 1 \dots \pm r,$

where  $z_i = 1 - 1/g_i n$ . The value of  $\sum A_k'$  is given in this case by the root of the equation

$$\frac{\sum A_k'}{2 \left( 1 + \sum A_k' \right)^2} + (2r + 1) \frac{\sum 1/g_k - (1/n) \sum g_k^{-2}}{\sum 1/g_k + n/2 \left( 1 + \sum A_k' \right)^2} = 2r + 1 - \frac{1}{n} \sum \frac{1}{g_k}.$$

The value of  $r$  is found by trial: for too large a value of  $r$ , several of the  $A_i$  turn out to be negative; if  $z_{r+1} > (1/n) \sum x_k / g_k$  then  $r$  must be increased.

To obtain an exact solution of (1) one must put in (2)

$$z_i = 1 - \frac{1}{g_i n} - C_i^2 \left[ 2 \left( 1 + \sum A_k' \right) \right]^{-4} \sum_{k,l} A_k' A_l' A_{k+l+i}' - C_i^3 \left[ 2 \left( 1 + \sum A_k' \right) \right]^{-6} \times \sum_{k,l,m,p} A_k' A_l' A_m' A_p' A_{k+l+m+p+i}' - \dots$$

<sup>5)</sup>The relationship  $\left[ 1 + \sum A_k' (1 - \cos 2\pi m_k x) \right]^{-1} \approx 1 - \sum A_k' (1 - \cos 2\pi m_k x)$  is used in<sup>[9]</sup>.

$\frac{\Delta\nu_{\text{fl}}}{c/2\pi l}$	n	Solution	$A_0$	$A_1$	$A_2$	$A_3$	$A_4$	$A_5$	$A_6$	$A_7$	$A_8$	$A_9$	$A_{10}$
6.8	3	exact	0.84	0.49	0								
		approx.	0.87	0.48	0								
	10	exact	3.4	2.6	0								
		approx.	3.8	2.5	0								
45	3	exact	0.27	0.26	0.24	0.19	0.13	0.04	0				
		approx.	0.29	0.28	0.25	0.19	0.11	0.01	0				
		using the method of <sup>[9]</sup>	0.130	0.129	0.126	0.120	0.113	0.102	0.090	0.073	0.053	0.029	0.001

(for  $|k| > rA'_k \equiv 0$ ;  $C_m^l$  is a number of combinations of  $m$  things taken  $l$  at a time); in this way we obtain the solution of the equations by iteration.

In the table we give the results of the calculation for a Lorentz fluorescence line shape for the case in which the half-width of the fluorescence line is either 6.8 or 45 times larger than the separation between the neighboring bands; this corresponds to rods of  $\text{CaF}_2:\text{Sm}^{2+}$  20 mm in length at temperatures 15 and 40°K. As is clear from the numbers in the table, even for a ten-fold excess above threshold the approximation used is completely applicable, whereas the formulas of Tang et al. are essentially unusable even for  $n = 3$ .

71 (1964), Soviet Phys. JETP 19, 51 (1964).

<sup>7</sup>Anan'ev, Galaktionova, Mak, and Sedov, Optika i spektroskopiya 16, 911 (1964).

<sup>8</sup>T. I. Kuznetzova and S. G. Rautian, FTT 5, 2105 (1963), Soviet Phys. Solid State 5, 1535 (1964).

<sup>9</sup>Tang, Statz, and DeMars, J. Appl. Phys. 34, 2289 (1963).

<sup>10</sup>Yu. Anan'ev and A. A. Mak, Optika i spektroskopii).

<sup>11</sup>W. R. Bennett, Phys. Rev. 126, 580 (1962).

<sup>12</sup>B. Z. Malkin, FTT 5, 1062 (1963), Soviet Phys. Solid State 5, 773 (1963).

<sup>13</sup>Iu. Anan'ev and A. A. Mak, Optika i spektroskopiya 16, 1065 (1964).

<sup>14</sup>H. Statz and C. L. Tang, J. Appl. Phys. 35, 1377 (1964).

<sup>15</sup>G. R. Hanes and B. P. Stoitcheff, Nature 195, 587 (1962).

<sup>16</sup>V. V. Korobkin and A. M. Leontovich, JETP 44, 1847 (1963), Soviet Phys. JETP 17, 1242 (1963)

<sup>17</sup>B. I. McMurtry, Appl. Opt. 2, 767 (1963).

<sup>18</sup>M. S. Lipsett, and M. W. P. Strandberg, Appl. Opt. 1, 343 (1962).

<sup>1</sup>D. F. Nelson and W. S. Boyle, Appl. Opt. 1, 181 (1962).

<sup>2</sup>P. P. Feofilov, Optika i spektroskopiya 1, 992 (1956).

<sup>3</sup>Kaiser, Garrett, and Wood, Phys. Rev. 123, 766 (1961).

<sup>4</sup>L. A. Vaĩnshteĩn, JETP 44, 1050 (1963), Soviet Phys. JETP 17, 709 (1963).

<sup>5</sup>G. D. Boyd and I. P. Gordon, Bell Syst. Techn. J. 40, 489 (1961).

<sup>6</sup>A. M. Leontovich and A. P. Veduta, JETP 46,

Translated by J. A. Armstrong